

# CHARACTERIZING QUANTUM LIGHT SOURCES VIA THE HANBURY BROWN AND TWISS EFFECT

Thanapat PHETVONGSAKUL<sup>1</sup>, Jeerasak PHU-ARPHIT<sup>1</sup>, Ruchipas BAVONTAWEEPANYA<sup>1</sup>,  
Atirach RITBOON<sup>1</sup> and Ekkarat PONGOPHAS<sup>1\*</sup>

<sup>1</sup> Division of Physics, Faculty of Science and Technology, Thammasat University,  
Thailand; e\_pong@tu.ac.th (Corresponding Author)

## ARTICLE HISTORY

**Received:** 9 June 2025

**Revised:** 23 June 2025

**Published:** 7 July 2025

## ABSTRACT

Quantum light sources is an essential element in various applications in quantum optics and quantum information, including quantum information processing, quantum computing, and quantum cryptography. The quality and nature of a light sources are defined by their characteristics which determines their efficiency in quantum applications and processing. In quantum optics, the second-order correlation function,  $g_{2D}^{(2)}(0)$ , is a key characteristic of quantum light sources. It is typically measured by the coincidence of signals from two spatially separated detectors in a Hanbury Brown and Twiss (HBT) setup. However, this method is not suitable for bidirectional quantum light sources. In this research, we characterized a bidirectional quantum light source by measuring the conditioned second-order correlation function  $g_{3D}^{(2)}(0)$  from the time delays of two photons in one arm triggered by signals of photons on another arm in a “gated HBT” setup. The light source is generated by the spontaneous parametric down-conversion (SPDC) process in a beta barium borate (BBO) crystal, pumped by a 405-nm continuous-wave laser. This light source, as a result, achieves  $g_{3D}^{(2)}(0) = 0.0437$ , demonstrating the efficiency of our experimental setup for generating a quantum light in an optical laboratory.

**Keywords:** Hanbury Brown and Twiss Effect, Second-order Correlation, Spontaneous Process Down-Conversion, Beta Barium Borate Crystal

**CITATION INFORMATION:** Phetvongsakul, T., Phu-arphit, J., Bavontaweepanya, R., Ritboon, A. & Pongophas, E. (2025). Characterizing Quantum Light Sources via the Hanbury Brown and Twiss Effect. *Procedia of Multidisciplinary Research*, 3(7), 45.

## INTRODUCTION

Single-photon sources are a crucial part of most protocols in quantum communication (Bouwmeester et al., 1997; Tittel & Weihs, 2001), quantum optics (Pittman et al., 2002), quantum computing (Walther et al., 2005) and quantum cryptography (Irvine et al., 2004). To achieve a single-photon light source, a well-known method generally uses a heralded single-photon source generated by a spontaneous parametric down-conversion (SPDC) process in a nonlinear crystal. The down conversion generates a pair of photons in two beams, called idler and signal. A heralded photon in the idler beam is used as a triggered signal to announce a single photon in the signal beam regarded as the single-photon source (Rarity et al., 1987). This element is fundamental to the infrastructure of quantum information technology.

The characteristic of a single-photon source defines its quantum nature and determines its efficiency in quantum applications. Typically, the second-order correlation function ( $g^{(2)}(0)$ ) was used to characterize quantum light sources (Beck, 2007; Blauensteiner et al., 2009; Bocquillon et al., 2009; Razavi et al., 2009; Thorn et al., 2004). A light beam from the quantum source is sent into a Hanbury Brown and Twiss setup. The correlation function then measured by the coincidence of signals from two detectors at the output ports of a beam splitter. The correlation function from this method is known as the two-detector correlation function,  $g_{2D}^{(2)}(0)$  (Beck, 2007; Thorn et al., 2004). The light source with  $g^{(2)}(0) < 1$  exhibits the photon antibunching and indicates the particle-like behavior (Reid & Walls, 1986).

However, for a two-beam quantum light source, this type of measurement requires more specific description. Two-detector correlation function can be measured between two beams, called “cross correlation”, or measured through only one beam, called “autocorrelation”. Moreover, one can insert another beam splitter in the signal beam in our setup, and measure a three-detector correlation function  $g_{3D}^{(2)}(0)$ , called “conditional autocorrelation” of one beam conditioned by signal from another beam.

In this research, we characterized a heralded-quantum-light source from SPDC process in a nonlinear crystal by measuring the cross-correlation between the idler and signal beams, the autocorrelation of the signal beam, as well as the conditioned autocorrelation of the signal beam conditioned by the signal from idler beam.

## METHODS

A single photon light source was produced by the SPDC process in a  $5\text{mm} \times 5\text{mm} \times 5\text{mm}$  type-I beta barium borate (BBO) crystal. This crystal was pumped by a 20-mW, 405-nm laser. The idler and signal beams are emitted at  $\pm 3^\circ$  with respect to the pump beam with the wavelength of 810 nm. These down-converted photons were detected by avalanche photodiode detectors (APD) placed in different locations as shown in the experimental setup, Figure 1. The detector placed in the idler arm is regarded as a gate detector (G detector). The detection of the idler photon heralds the presence of the single signal photon in the signal arm. The signal beam passes through the Hanbury Brown and Twiss (HBT) setup, including a 50:50 beam splitter (BS) to split the beam and two APDs located at the outputs of the beam splitter, labelled R detector and T detector as shown in Figure 1(A). A time tagging module was used to measure all possible signals including the single count rate at each detector, *i.e.* G-, R-, and T-count rate, and the coincidence count rate, *i.e.* GR-, GT-, RT-, and GTR-count rate.

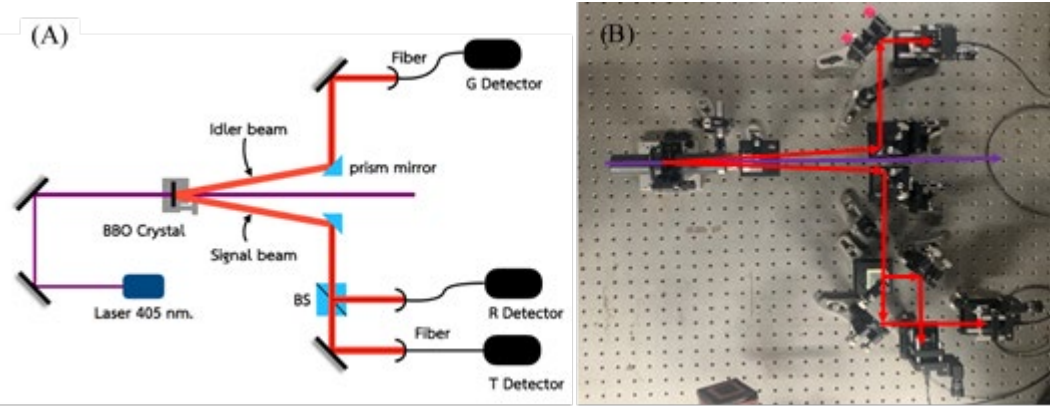


**Figure 1** (A) The schematic optical setup designed for analyzing the characteristics of a quantum light source. (B) A photograph of the optical setup in the laboratory.

To analyze the characteristics of a quantum light source, we measured the cross-correlation between the G detector and either the R or T detector. The G detector's signal served as a trigger to start the clock, while the R or T detectors' signal was used to stop the clock. These start-stop signals with different time intervals were collected over time and plotted on a histogram to illustrate the relation of the coincidence signals and the time intervals in Figure 2. The height of the peaks in the histogram shows the production rate of photon pairs from the BBO. Next, we measured the autocorrelation of the signal beam by counting start-stop signals between the R and T detectors at various time intervals and determined the second-order correlation function  $g_{2D}^{(2)}(0)$  as shown in Figure 3. Additionally, we measured both two-fold coincidences (between G and either R or T), three-fold coincidences (G, R, and T detectors), and the total number of signal counts at the G detector. These data enabled us to investigate the photon bunching behavior of our quantum light source and calculate the conditional second-order correlation function  $g_{3D}^{(2)}(0)$ . Finally, the conditional time-correlated signals of the signal beam were measured. The coincidence of signals from the G and R detectors were used to start the clock which was then stopped by the signal from the T detector. The histogram of conditional time-correlated signals at different times is shown in Figure 5 which illustrates the photon bunching behavior of this light source.

## RESULTS & DISCUSSION

From Figure 2, the measured cross-correlation has peaks located at the time delay of 10.4 nanoseconds and 22.4 nanoseconds corresponding to the path difference of the light beams verifying the generation of down-converted photon pairs from the BBO. The blue line represents the correlation between a photon in idler beam reaching the G detector and that in signal beam reaching to the R detectors. Similarly, the orange line represents the correlation between the G and T detectors. The number of produced photon pairs is represented by the number of coincidence counts at both peaks, due to the nature of the SPDC process in BBO crystal, when a pump photon is absorbed and re-emitted as the down-converted with a lower energy (Hong & Mandel, 1985). This means, if a down-converted photon reaches the G detector, its counterpart should reach either the R or T detectors at a specific time delay depending on the optical path difference. These two peaks have the maximum values of 9,440,414 and 9,778,810 counts, respectively.

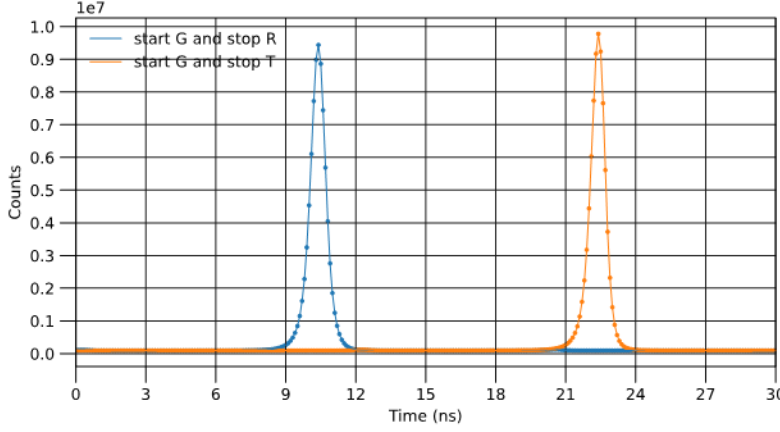


**Figure 2** The histogram shows start-stop signals at different time delays. The blue (orange) line represents the coincidence of G and R detectors (G and T detectors). The coincidences had been collected for 3 hours with a resolution of 100-ps.

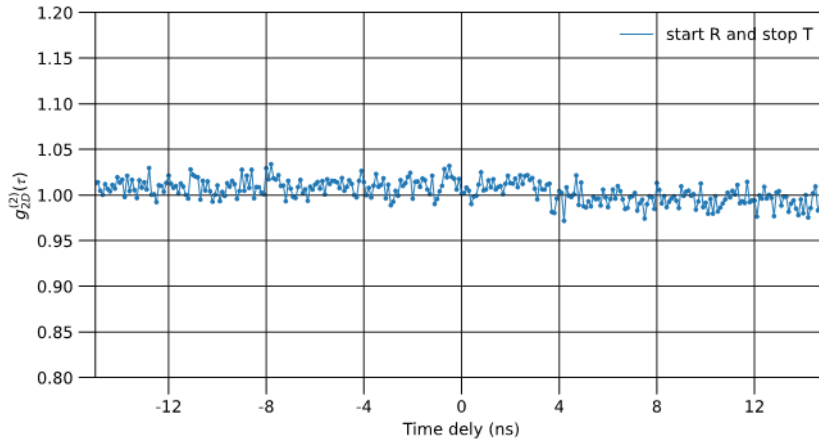


**Figure 3** The histogram shows the  $g_{2D}^{(2)}(\tau)$  signals between the R and T detectors at different time delays. The data had been collected for 1 hour with a resolution of 100-ps.

In Figure 3, we obtained the autocorrelation of the signal beam by measuring the  $g_{2D}^{(2)}(\tau)$  signals between the R and T detectors at different time delays. The measured values were consistently around 1 indicating that after a photon arrives at the R detector, another photon can reach the T detector at any time delay. This autocorrelation, of course, cannot be considered as an evidence of the photon anti-bunching of the light source, as it does not exhibit a trough at zero time delay. This implies that the SPDC light source demonstrates behavioral evidence of photon bunching, when neglecting the signal from the heralded photon (Blauensteiner et al., 2009; Bocquillon et al., 2009; Razavi et al., 2009). Next, we measured the conditioned second-order correlation function  $g_{3D}^{(2)}(0)$ , by counting the coincidences in which the G, R, and T detectors triggered simultaneously. Then, the two-fold coincidences of G and either R or T detectors were counted. The coincidence window was set to be 500 picoseconds over a data collection period of 3 hours. Additionally, we measured the number of single counts at the G detector. The two-fold coincidence counts between G and R detectors (GR) was 42,456,201, and that between G and T detectors (GT) was 43,578,789. The three-fold coincidence count, on the other hand, was 15,574, and the single count at the G detector was 5,191,051,612.

In this Venn diagram of Figure 4, area (a) illustrates the number of events that triggered only the G and R detectors, which was 42,440,627, and area (c) represents those that triggered only the G and T detectors, which was 43,563,215. Area (b) represents the number of three-fold

coincident events of all detectors (G, R, and T), with a total of 15,574 counts. These three-fold coincident events reflect the probability of producing photon bunching in the light source.

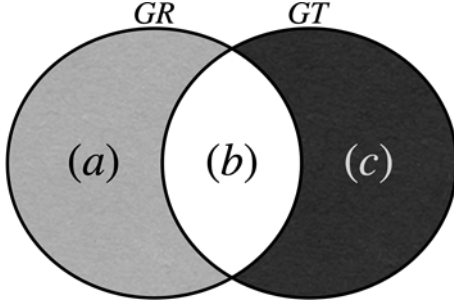


**Figure 4** The Venn diagram classifies the two-fold coincidence counts of G and either R or T detectors. The intersecting area (b) represents the three-fold coincidence counts of the three detectors.

The conditional second-order correlation function  $g_{3D}^{(2)}(0)$  is defined as (Beck, 2007; Thorn et al., 2004),

$$g_{3D}^{(2)}(0) = \frac{P_{GTR}(0)}{P_{GT}P_{GR}}, (1)$$

where  $P_{GTR}(0)$  is the probability of detecting photons at the G, T and R detectors with different coincidence windows,  $P_{GT}$  is the probability of detecting photons at G and T detectors, and  $P_{GR}$  is the probability of detecting photons at G and R detector within the assigned coincidence window. These probabilities can be determined from the signal counts as (Malygin et al., 1891; Penin & Sergienko, 1991)

$$P_{GTR} = \frac{N_{GTR}}{N_G}, P_{GT} = \frac{N_{GT}}{N_G}, P_{GR} = \frac{N_{GR}}{N_G}, (2)$$

where  $N_{GTR}$  is the number of coincidence counts of the three detectors in within the coincidence window,  $N_{GT}$  is the number of coincidence counts at the G and T detector,  $N_{GR}$  is the number of coincidence counts at the G and R detector, and  $N_G$  is the number of signal counts of the G detector. From Equation 2, we can rewrite the  $g_{3D}^{(2)}(0)$  in Equation. (1) as

$$g_{3D}^{(2)}(0) = \frac{N_{GTR}N_G}{N_{GT}N_{GR}}. (3)$$

This gives the achieved conditioned second-order correlation function at zero time delay to be  $g_{3D}^{(2)}(0) = 0.0437$ . This very low value of  $g_{3D}^{(2)}(0)$  supports a strong photon anti-bunching, indicating that a photon that arrives at the G detector heralds the presence of an emitted photon pair. This postselection process, therefore, enables the signal beam to behave as a quantum light source as desired.

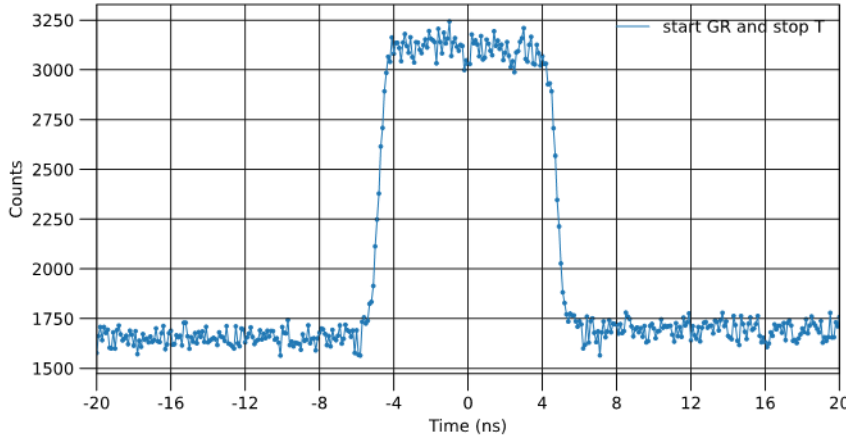


**Figure 5** This histogram shows the conditioned start-stop signals of the signal beam, obtained when two photons are detected simultaneously at the G and R detectors and another photon is detected later at the T detector at various time delays. The data was collected over 3 hours with a time resolution of 100 ps.

Finally, to validate the photon bunching feature of the light source, we employed a heralded photon method to conditionally measure the start-stop signals of the signal beam. As shown in Figure 5, photon bunching is reflected by a clear peak located at zero time delay, with a consistent count of approximately 3,100, nearly twice as high as the counts at other time delays. This indicates that after two photons are detected simultaneously at the G and R detectors, a third photon, if it does exist, is likely to arrive at the T detectors within a short temporal window near zero time delay. This result confirms the existence of photon bunching behavior, which is characteristic of a quantum light source.

## CONCLUSION

The quantum light source from SPDC process is characterized using cross-correlation measurements of the down-converted photon pairs. The unconditioned second-order correlation function  $g_{2D}^2(0)$  in one arm remains consistently around 1, which is insufficient to demonstrates the wave-like behavior of the light in one arm. In contrast, the conditioned second-order correlation function  $g_{3D}^2(0)$ , measured by using a heralded photon method, achieved a very low  $g_{3D}^2(0)$  with the value of 0.0437. This reveals strong photon anti-bunching which is considered as a clear signature of non-classical light. The heralded photon method, as a result, allows the post-selection process to effectively achieve the single photon light source. However, a significant number of the three-fold coincident events and the apparent peak located at zero time delay confirm the existence of photon bunching behavior, indicating a non-negligible probability of multi-photon generation via the SPDC process and reinforcing the fact that the source does not emit only single photon pairs.

## ACKNOWLEDGEMENTS

This work is supported by Research Program supported by the Faculty of Science and Technology Thammasat University (Scholarship for talent student to study graduate program), Thailand. Contract No.TB 38/2565

## REFERENCES

Beck, M. (2007). Comparing measurements of  $g^{(2)}(0)$  performed with different coincidence detection techniques. *J Opt Soc Am B*, 24(12), 2972.

- Blauensteiner, B., Herbauts, I., Bettelli, S., Poppe, A., & Hübner, H. (2009). Photon bunching in parametric down-conversion with continuous-wave excitation. *Phys Rev A*, 79(6).
- Bocquillon, E., Couteau, C., Razavi, M., Laflamme, R., & Weihs, G. (2009). Coherence measures for heralded single-photon sources. *Phys. Rev. A*, 79, 035801.
- Bouwmeester, D., Pan, J. W., Mattle, K., Eibl, M., Weinfurter, H., & Zeilinger, A. (1997). Experimental quantum teleportation. *Nature*, 393, 215-221.
- Hong, C. K., & Mandel, L. (1985). Theory of parametric frequency down conversion of light. *Phys Rev A*, 31(4), 2409-18.
- Irvine, W. T. M., Linares, A. L., de Dood, M. J. A., & Bouwmeester, D. (2004). Optimal Quantum Cloning on a Beam Splitter. *Phys. Rev. Lett*, 92, 047902.
- Malygin, A. A., Penin, A. N., & Sergienko, A. V. (1981). Absolute calibration of the sensitivity of photodetectors using a biphotonic field. *JETP Lett*, 10, 493-496.
- Penin, A. N., & Sergienko, A. V. (1991). Absolute standardless calibration of photodetectors based on quantum two-photon fields. *Appl. Opt*, 30, 3582-3588.
- Pittman, T. B., Jacobs, B. C., & Franson, J. D. (2002). Single photons on pseudodemand from stored parametric down-conversion. *Phys. Rev. A*, 66, 042303.
- Rarity, J. G., Ridley, K. D., & Tapster, P. R. (1987). Absolute measurement of detector quantum efficiency using parametric down conversion. *Appl. Opt*, 26, 4616-4619.
- Razavi, M., Söllner, I., Bocquillon, E., Couteau, C., Laflamme, R., & Weihs, G. (2009). Characterizing heralded single-photon sources with imperfect measurement devices. *J Phys B: At Mol Opt Phys*, 42(11), 114013.
- Reid, M. D., & Walls, D. F. (1986). Violations of classical inequalities in quantum optics. *Phys. Rev. A*, 34, 1260-1276.
- Thorn, J. J., Neel, M. S., Donato, V. W., Bergreen, G. S., Davies, R. E., & Beck, M. (2004). Observing the quantum behavior of light in an undergraduate laboratory. *American Journal of Physics*, 72, 1210-1219.
- Tittel, W., & Weihs, G. (2001). Photonic entanglement for fundamental tests and quantum communication. *Quant. Inf. Comput*, 1, 3-56.
- Walther, P., Resch, K. J., Rudolph, T., Schenck, E., Weinfurter, H., Vedral, V., Aspelmeyer, M., & Zeilinger, A. (2005). Experimental one-way quantum computing. *Nature*, 434, 169-176.

**Data Availability Statement:** The raw data supporting the conclusions of this article will be made available by the authors, without undue reservation.

**Conflicts of Interest:** The authors declare that the research was conducted in the absence of any commercial or financial relationships that could be construed as a potential conflict of interest.

**Publisher's Note:** All claims expressed in this article are solely those of the authors and do not necessarily represent those of their affiliated organizations, or those of the publisher, the editors and the reviewers. Any product that may be evaluated in this article, or claim that may be made by its manufacturer, is not guaranteed or endorsed by the publisher.



**Copyright:** © 2025 by the authors. This is a fully open-access article distributed under the terms of the Attribution-NonCommercial-NoDerivatives 4.0 International (CC BY-NC-ND 4.0).